N73-16834

NASA TECHNICAL MEMORANDUM

NASA TM X-62,226

NASA TM X-62,226

CASE FILE COPY

NIGHTSIDE ELECTROMAGNETIC RESPONSE OF THE MOON

G. Schubert
University of California, Los Angeles, Calif. 90024

B. F. Smith, C. P. Sonett, D. S. Colburn
Ames Research Center, Moffett Field, Calif. 94035

K. Schwartz
20858 Collins Street
Woodland Hills, Calif. 91364

October 1972

THE NIGHT SIDE ELECTROMAGNETIC RESPONSE OF THE MOON

G. Schubert

Department of Planetary and Space Science
University of California, Los Angeles
90024

B. F. Smith, C. P. Sonett, D. S. Colburn

National Aeronautics & Space Administration
Ames Research Center
Moffett Field, California
94035

K. Schwartz

20858 Collins Street
Woodland Hills, California
91364

October, 1972

ABSTRACT

The electromagnetic response of the Moon to excitation by the time dependent fluctuations of the interplanetary magnetic field is given for the dark or antisolar hemisphere of the Moon. Six hours of time series data from the Explorer 35 Ames magnetometer and the lunar surface magnetometer on Apollo 12 are used to obtain the Fourier spectral amplitudes of the surface and interplanetary fields from which transfer functions are calculated for the east-west, north-south, and vertical directions at the Apollo site in the bandwidth $1.7 \times 10^{-3} \leq f \leq 3 \times 10^{-2}$ Hz. The tangential magnetic field on the night side hemisphere is amplified by confinement within the diamagnetic cavity and redistribution of magnetic field lines from the sunlit to the night side. Vacuum scattering from even a perfectly conducting Moon cannot produce the observed night side tangential magnetic field amplification. The night side electromagnetic behavior of the Moon is not that of a body in vacuum. A critical discussion of lunar conductivity profiles derived from night side radial magnetic field data and vacuum scattering theory is presented. Limitations imposed by the quantity and the frequency range of the data and the necessity to account for contributions from cavity confinement and internal redistribution of field

lines to the night side radial field make heretofore derived night side conductivity profiles unreliable. In particular, we show that there is no evidence for a lunar core as conducting as 10^{-2}mhos/m. Inversion of night side radial magnetic field data should await the development of a time-dependent asymmetric theory of lunar magnetic induction.

INTRODUCTION

The inductive response of the Moon to interplanetary magnetic field fluctuations has been measured by the Apollo 12 lunar surface magnetometer both when the instrument was on the lunar day (e.g. Sonett et al., 1972) and night sides (e.g. Dyal et al., 1972). Reports of the night side inductive response have been limited to analyses of a number of individual transient events. The latter work has concentrated mainly on the night side response of the radial magnetic field near the antisolar point. It has been assumed in studying these night side transients, that the Moon's night side radial response to step changes in the interplanetary magnetic field was similar to that of a conducting sphere in vacuum. However, this assumption has not been quantitatively tested by the field observations themselves.

In this paper we report the dependence of the night side lunar response on frequency in the band from about 10^{-3} to 10^{-2} Hz. Both the behavior of the radial and tangential magnetic fields are analyzed based on a larger quantity of data than hitherto considered. We show from the data the the night side response of the Moon is not that of a sphere in vacuum. Instead, hydromagnetic radiation scattered from the Moon is strongly confined to the interior of the cavity formed downstream from the Moon in the solar wind. Scattered electromagnetic fields can be expected to occupy the space within the downstream boundary of the conical surface tangent to the lunar limb and making the Mach angle with the supermagnetosonic solar wind. The cavity confinement of the induced lunar magnetic field is clearly seen in the large amplification of fields which are tangent to the lunar surface, whereas the effect of the cavity on the radial magnetic field is less obvious.

In a series of papers Sonett et al. (1971a, b; 1972), using transfer functions derived from data obtained on the sunlit side of the Moon, have derived a model of the lunar conductivity with a core of radius about 1200 km and conductivity several times 10^{-3}mhos/m and an intermediate layer extending out as far as 1650 km with a conductivity of several times 10^{-4}mhos/m. (The conductivity "spike" reported in Sonett et al. (1971a, b) is shown in Sonett et al. (1972) to be a member of a set of conductivity models all having similar equivalent electrical response including the monotonic profile discussed here.) This intermediate layer is in turn surrounded by an outer crust whose conductivity is too low to be presently resolved by the surface magnetometer experiment. Dyal and Parkin (1971a, b) and Dyal et al. (1972) have analyzed individual transient events observed on the dark lunar hemisphere and have derived lunar conductivity models with a core of radius $\approx$1000 Km and conductivity of $\approx 10^{-2}$mhos/m surrounded by an intermediate layer extending out to about 1650 km with a conductivity of about

3×10^{-4}mhos/m. These models derived from two different bodies of data and using two different theoretical approaches, are quite similar. The differences in the core conductivities translates to a difference of only a few hundred degrees in the deep lunar temperature. However, the higher temperature associated with the more conducting core is in the range where solid state convection may contribute to the cooling of the lunar interior, whereas at the lower temperature convection would be unlikely. For this reason a resolution of the relatively small deep conductivity difference is important. We therefore present a discussion of lunar conductivity models derivable from vacuum theory inversion of night side radial magnetic field data. Aside from questions of uniqueness and applicability of vacuum theory, we will show that a core of conductivity 10^{-2}mhos/m and radius 1000 km cannot be inferred from the night side data simply because it is not resolvable from the data.

In forthcoming papers (Schubert et al., 1972; Smith et al., 1972) we will report the dependence of the lunar response on surface position using both theory and observation. Until now, the lunar inductive response has been viewed from two disparate theoretical points of view, i.e. spherically symmetric plasma and vacuum theories, and the theories applied to two separate bodies of data, sunlit side and night side observations. This is the first in a series of papers which is intended to unify theoretical and observational understanding of the Moon as a body scattering electromagnetic radiation into an asymmetric plasma environment.

DATA

This section gives the first report of the electromagnetic response of the Moon as a function of frequency obtained from the Apollo 12 Lunar Surface Magnetometer (LSM) and the Ames magnetometer on the Explorer 35 Lunar Orbiter, while the LSM was in lunar darkness. The three transfer functions A_x, A_y, and A_z are shown in Figure 1 as a function of frequency f for 1.66×10^{-3} Hz $\leq f \leq$ 2.98×10^{-2} Hz. The transfer functions are defined as in earlier papers (Sonett et al., 1971a, b; Sonett et al., 1972) which discussed the sunward hemisphere lunar response

$$A_i(f) = [h_{2i}(f) + h_{1i}(f)]/h_{1i}(f) \qquad (1)$$

where the sum $h_{2i} + h_{1i}$ is the Fourier transform of the magnetic field measured by LSM and h_{1i} is the Fourier transform of the field measured by the Explorer 35 magnetometer. The coordinates are identical with those employed before, with x vertical, y positive eastward, and z positive northward at the LSM site.

To obtain the data shown in Figure 1 we used 6 one hour time series swaths carefully combed for noise and data gaps. Since the Explorer 35 magnetometer bandwidth is substantially less than that of the LSM, data from the latter was decimated and both data sets filtered in accordance with procedures discussed elsewhere (Sonett et al., 1971b). *The Explorer 35 data used in this paper* was taken while the lunar satellite was free of any obvious influence from the Moon and while it and the Moon were both free of the Earth's magnetosphere, magnetosheath, and geomagnetic tail. We will show elsewhere (Schubert et al., 1972; Smith et al., 1972) that the transfer functions are sensitive to solar longitude (local time on the Moon). This dependence is especially marked in the vicinity of the limb. Thus, we have used data taken only while the LSM is within 45^{o} of the anti-solar point, a longitude interval which is a compromise between an effort to maximize the distance from the lunar terminator and diamagnetic cavity walls and minimize the standard deviations in the transfer function data. We still expect an influence from the angular dependence of the response functions. Dyal and Parkin (1971a, b) who analyzed magnetic transients on the night side of the Moon, restricted their data set to a similar longitude interval.

Each data point and each error estimate in Figure 1 are based upon the mean and standard deviation of the means of the individual transfer functions of the one hour time series records. The magnitudes of the errors are related to the restriction of the data set by the requirement of limited longitude. The general appearance of the transfer functions is distinct from that obtained for the sunward hemisphere of the Moon. This is not surprising since the confining effects of the solar wind dynamic pressure (Sonett et al., 1971c) are absent on the dark side of the Moon. The A_y and A_z tangential transfer functions show approximately constant response between 1.66×10^{-3} Hz and 10^{-2} Hz, with a decrease at higher frequency. For the whole spectral interval $A_z > A_y$. The radial transfer function A_x shows an approximately monotonic decrease with increasing frequency from a value near unity at the lowest frequency.

COMPARISON OF DATA WITH VACUUM RESPONSE OF SIMPLE LUNAR MODELS

The spherically symmetric vacuum response of several lunar models is shown together with the data in Figure 2. For the purpose of this discussion, simple Moon models are adequate. The horizontal lines are the transfer functions for models with perfectly conducting cores of radius b surrounded by insulating shells of thickness a-b. The curves labelled with a value of electrical conductivity σ are the transfer functions for models wherein σ is constant. The theoretical transfer functions greater than unity are for the tangential field (either north-south or east-west since the symmetry of the theory yields identical transfer functions for both components) while those less than unity are for the radial magnetic field. The horizontal axis of the figure is in fact the radial transfer function for the model b/a = 1.0.

The low frequency tangential transfer function for any spherical body ($2\pi af/c << 1$, where c is the velocity of light in vacuum) scattering in a vacuum cannot exceed the value 1.5 attained by the perfectly conducting sphere. For models with perfectly conducting cores, the tangential transfer function decreases and the radial transfer function increases as the core size decreases. For uniformly conducting models, the tangential function increases monotonically from unity at f = 0 and the radial function decreases monotonically from unity at f = 0.

For $f \simeq 0.01$ Hz the observed values of the tangential response are in excess of the theoretical maximum of 1.5. Sill (1972) has noted that the observed tangential response of a transient observed on the lunar night side exceeds that which would be predicted by spherically symmetric vacuum theory. According to the radial transfer function data the Moon behaves like a uniformly conducting sphere with $\sigma \approx 10^{-4}$ mhos/m. An iteratively derived model given below confirms this. However, the tangential transfer function for such a model bears no relationship to the experimental data. Moreover, the tangential transfer function data lie in the region unattainable by vacuum scattering from a spherical body. Indeed Figure 2 shows that for low frequency, i.e., $f \lesssim 0.01$ Hz, the tangential transfer functions attain values as large as 1.8, considerably in excess of the theoretical limit of 1.5, a low frequency maximum for the tangential response of a conducting body in a vacuum. Thus spherically symmetric vacuum theory is an inappropriate description of the electromagnetic scattering on the dark side of the Moon. The high value of the empirical tangential transfer function is due to amplification by cavity confinement of the induced magnetic field which is compressed into a space bounded by the front side lunar surface, the cavity boundary and the lunar skin depth profile and by redistribution of field lines from the sunlit to the night side (Schubert et al., 1972; Smith et al., 1972).

RESOLUTION OF LUNAR CONDUCTIVITY MODELS USING RADIAL DATA

The high value of the observed night side tangential response demonstrates unequivocally that vacuum theory does not describe the scattering of incident interplanetary magnetic fields on the lunar dark side hemisphere. Although the A_y and A_z transfer functions are modified by cavity amplification, it is not a priori clear how important the cavity contributions are to the radial transfer function in the neighborhood of the antisolar point.

The radial transfer function data A_x shown in Figure 1 have been inverted using spherically symmetric vacuum scattering theory and a three layer model of lunar electrical conductivity. Layer radii and electrical conductivities are determined iteratively (except for the outermost layer which is assumed to be insulating) by obtaining the best theoretical fit to the empirical A_x. The resolution obtainable with the present data set does not warrant a Moon model more complicated than a three layer one and possibly less as will be shown presently. The iteration for a best fit model was terminated when the variance in the fit of the iterated model was 1.6×10^{-2}. The variance of the data is 7.9×10^{-2}, showing that the resolution limit is determined by the data errors.

The model has a core of radius 1240 km and conductivity 2.9×10^{-4} mhos/m surrounded by a shell of conductivity 1.7×10^{-4} mhos/m whose outer radius is essentially the lunar radius R_m. The theoretical radial transfer function corresponding to the iterated conductivity model is shown overlaying the data in Figure 3. We also show in Figure 3 the tangential transfer function $A_y = A_z$ for this conductivity model superimposed upon the experimental data. At $f \lesssim 0.01$ Hz the observed values of the tangential response are clearly far in excess of this theoretical tangential transfer function consistent with the absolute limit imposed by vacuum theory upon any model. The derived model cannot even qualitatively simultaneously satisfy the radial and tangential data. This statement is true of any lunar conductivity model using vacuum scattering theory.

Models of electrical conductivity derived from inversion of A_x data are nonunique. The models reported by Dyal et al. (1972) used 11 transients; these were tracked for 10 minutes each giving a total data span of about 2 hours, as compared with the 6 hours used in this paper. The iterated model reported here should be a member of the set of possible profiles reported by Dyal et al. (1972) since our data set is three times as large as theirs. However, the core conductivity derived here is at least a factor of three less conducting than the least permissible core conductivity of similar size cores according to Dyal et al. (1972). In this connection we note that the variance in the fit of a typical model reported by Dyal et al. (1972) (core conductivity 10^{-2}mhos/m, core radius 0.6 R_m, shell conductivity $3x10^{-4}$mhos/m, and shell radius 0.95 R_m) is $4.6x10^{-2}$; this is within the variance of the data but a factor of three larger than the variance of our iterated model. The core and shell conductivities of the iterated model reported here differ by less than a factor of 2, implying a rather uniformly conducting Moon. A nearly uniform Moon provides an excellent fit to our larger data set whereas Dyal et al. (1972) require large conductivity variations approaching two orders of magnitude between core and shell to adequately fit their subset of data. On the basis of our inversion of A_x, there is no reason to require a core as conducting as that proposed by Dyal et al. (1972). In addition, it will be shown that the conductivity at depths of 800 km in the Moon cannot be estimated from the data of this paper and presumably also from the much smaller data set of Dyal et al. (1972). Since the inversion seeks a solution with minimum variance, it is entirely possible that physically unrealistic features, such as the coincidence of the outer radius of the conducting shell with the lunar radius itself, result from a solution whose variance is smaller than that of the data. To explore these points in more detail a number of additional calculations have been performed.

Figure 4 shows the effect of adding a highly conducting core to the uniform model derived here. The radial transfer function amplitude for a uniformly conducting Moon with $\sigma = 1.7 \times 10^{-4}$ mhos/m is shown together with the data in the figure and the fit is excellent (variance of fit $\approx 1.5 \times 10^{-2}$). Cores of conductivity 10^{-2} mhos/m and different radii are added to the uniform model and the radial responses of the new models are computed. For core radii less than 500 km the response is negligibly different from that of the uniform model. The radial response of the model with a core radius of 1000 km and conductivity of 10^{-2} mhos/m surrounded by a shell of conductivity 1.7×10^{-4} mhos/m is sufficiently different at the low frequencies to be shown in the figure. The variance of fit of the latter model is also $\approx 1.5 \times 10^{-2}$. It is clear that this model is indistinguishable from the uniformly conducting Moon in terms of variance of fit; both models have a variance a factor of 5 less than the data. A core of radius 1000 km and $\sigma = 10^{-2}$ mhos/m is not resolvable from the data reported here. Presumably it cannot be resolvable from the smaller data set used by Dyal et al. (1972). The radial response of a model with a core radius of 1200 km is also shown in the figure. Its variance of fit is 3.4×10^{-2}. If a highly conducting core this large were present in the Moon it would begin to be resolvable in the A_x data, clearly however the fit is a poorer one. Thus we conclude that inversion of the A_x data reported here using vacuum theory provides no indication of a highly conducting core in the Moon.

The model Moon with uniform conductivity $\sigma \approx 1.7 \times 10^{-4}$ mhos/m cannot realistically represent the true near surface lunar conductivity. From our knowledge of the electrical conductivity of geologic materials under physical conditions similar to those existing near the lunar surface we can conclude that the actual Moon possesses an outer shell of material sufficiently nonconducting to be considered insulating. Indeed, if the Moon were in fact as conducting as 10^{-4} mhos/m at the lunar surface, a bow shock would form when the Moon was in the supersonic solar wind (Sonett and Colburn, 1967). Lunar orbiting satellites have so far failed to detect such a shock (Colburn et al., 1967; Ness et al., 1967).

In Figure 5 we investigate the effect of adding insulating shells of varying thickness to an otherwise uniform Moon model. For an approximately 40 km thick shell, the variance of fit of the radial transfer function computed from vacuum theory is 4×10^{-2}, somewhat larger than that of the iterated (essentially uniform) model but well within the variance of the data. For a shell thickness of 90 km the variance of fit is 0.14 and for a 140 km thick shell it is 0.33. As the shell thickness increases the radial response decreases at all frequencies of interest. The modification of the response at low frequencies is analogous to the effect of the reduction of core conductivity and/or size. We must conclude that a nonconducting near surface region between 50 and 100 km thick is not resolvable from the radial data reported here.

EFFECT OF FINITE WAVELENGTH

Another complication in the interpretation of the near surface lunar conductivity profile is the failure of vacuum theory to include time dependent multipoles of order greater than dipole. This is the result of the unrealistically large wavelengths encountered in the vacuum description.

Straightforward application of spherically symmetric vacuum theory to the interpretation of dark side magnetic data tacitly implies that the phase velocities of incident and scattered radiation are equal to the speed of light. Thus all wavelengths are large compared to the scale size of the Moon and the response is recognized as lying wholly within the Rayleigh limit. It has been shown that the long wavelength approximation is in error for the high frequency lunar response where quadrupole and higher order multipole contributions make the lunar response dependent on the angle θ between the incident wave vector and the position of LSM (Schubert and Schwartz, 1972). The wave equation permits separate phase velocities to be specified for the incoming and outgoing radiation. Thus we may assign a phase velocity v_p to the incident wave field appropriate to disturbances travelling in the solar wind plasma while holding the outgoing speed equal to c, appropriate to waves scattered into a nonconducting cavity. In Figure 6 we show transfer functions which include all significant time dependent multipoles. The conductivity model used to determine these transfer functions is the iterative solution given earlier in this paper. Calculations are shown for a number of scattering angles θ. The phase velocity, v_p = 300 km/sec is based on the assumption that the direction of the incident wave is along the idealized Parker spiral direction (Belcher and Davis, 1971). Clearly the variation in response with θ at high frequency complicates a determination of the near surface conductivity profile. Thus the incident wave vector spectrum must be included in the inversion of all magnetic field data in order to specify the conductivity at shallow depths in the Moon.

COMMENTS ON PREVIOUSLY REPORTED CONDUCTIVITY MODELS

In this section we calculate and then discuss the vacuum radial responses of lunar conductivity models previously derived from analysis of individual night side transients (Dyal and Parkin, 1971b; Dyal et al., 1972) and from sunlit side magnetometer data (Sonett et al., 1971b, 1972). The vacuum radial transfer functions of two night side transient models are shown together with the data in Figure 7. The models have a core conductivity of 10^{-2}mhos/m with a core radius of 1044 km, and intermediate shells of conductivity 10^{-4} (Model D1) and 3×10^{-4}mhos/m (Model D2) with thickness 606 km surrounded by insulating outer layers. We recall from the previous section that such a core is not in fact resolvable from the A_x night side data.

To emphasize this we have also shown in Figure 7 the effect on the response of reducing the core conductivity of Model D2, holding other parameters of the model fixed. If the core conductivity is reduced from 10^{-2}mhos/m to 3×10^{-3}mhos/m the change in response is so negligible that it could not be distinguished from the response of Model D2. The curve labelled D2(a) is the response of models with core conductivity reduced to

10^{-3} and 5×10^{-4}mhos/m, and the one labelled D2(b) is the response for a model with core $\sigma = 10^{-5}$mhos/m. The variances of fit of the responses of Model D2 and all its modifications presented here are all nearly 0.05. Clearly a highly conducting core is not resolvable from the data. It is interesting that the response, at the lowest frequency, of the model modification with the least conducting core is the best fit to the data! This should be contrasted with the claim of Dyal et al. (1972) that a highly conducting core is required to match the lunar response at long times (10 minutes).

That the outer insulating shell is also not fully resolvable is clear from the results of Figure 5 and the absence of finite wavelength effects in vacuum theory. This latter effect has been discussed by Schubert and Colburn (1971) who showed that the finite time of even a perfect discontinuity to transit the Moon makes a ramp input rising in say 10-15 seconds a more realistic approximation to the forcing function of a typical night side radial transient. The fit of the model with shell conductivity 10^{-4}mhos/m (D1) is poor; its variance of fit is 0.56. A change of only a factor of 3 in this shell conductivity (Model D2) leads to an acceptable fit with a variance of 0.046!

ARBITRARINESS OF THEORY IN MODEL BUILDING

The validity of conductivity models is ultimately based upon the correctness of the theory which is inserted in model fitting or inversion computations. As an example, in the case of iterative inversions the only computational requirement upon the theory is that it provide convergent iteration. This is a subtle requirement and sometimes is not met even for correct theory except in local neighborhoods in the solution space.

To see qualitatively the meaning of these statements with respect to the relative freedom of choice of theory we recall that model construction in general requires comparison of a response based upon an assumed model, followed by correction of the model toward ones showing convergence of the sum of the squared residues. Thus the theory is arbitrary so long as convergence is satisfied; the model set is at best unique only within the theoretical statement, and of course often not unique even then.

The conclusion to be drawn is that the validity of the theory used for model building has no intuitive connection with the "goodness" of fit; poor theory can yield an excellent fit to data, but the derived model is poor. Models based upon plasma confinement theory can provide self-consistent response approximations to front side lunar data as can models using vacuum theory together with dark side radial data. Yet the final models are different in that the night side derived vacuum model is uniformly conducting while the sunlit side plasma confined model is more conducting in its interior. The difficulty is in the application of vacuum theory which is known from the physics of the problem to be a poor statement of the theoretical night side response of the Moon. Indeed vacuum theory should be rejected on the grounds that it cannot provide a self-consistent description of radial and tangential responses.

In choosing between conductivity models for the Moon the required guide must be the error residue of the data set specified rigorously by the standard errors, the distribution law for the errors, and finally the theory used in the iteration loop. From the quasistatic asymmetric theory of Schubert et al. (1972) and the results of this paper, it is already clear that vacuum theory is unacceptable for insertion into an iterative loop based upon the dark side tangential response function, because the experimental response lies outside the domain of solutions provided by vacuum theory. This is an obvious constraint. For the radial function, vacuum theory is in error because of the asymmetric response and also because of the neglect of the higher order multipoles excited in the Moon. These are known to be important at the high frequency end of the spectrum from the non-monotonicity of the sunward hemisphere transfer function.

ACKNOWLEDGMENT

This work was supported in part by NAS 2-6876.

REFERENCES

Belcher, J. W., and L. Davis, Large amplitude Alfvén waves in the interplanetary medium, J. Geophys. Res., 76, 3534-3563, 1971.

Colburn, D. S., R. G. Currie, J. D. Mihalov, and C. P. Sonett, Diamagnetic solar wind cavity discovered behind Moon, Science, 158, 1040-1042, 1967.

Dyal, P., and C. W. Parkin, Electrical conductivity and temperature of the lunar interior from magnetic transient response measurements, J. Geophys. Res., 76, 5947-5969, 1971a.

Dyal, P., and C. W. Parkin, The Apollo 12 magnetometer experiment: Internal lunar properties from transient and steady magnetic field measurements, Proc. of the Second Lunar Sci. Conf., Vol. 3, 2391-2413, The M. I. T. Press, 1971b.

Dyal, P., C. W. Parkin, and P. M. Cassen, Surface magnetometer experiment: Internal lunar properties and lunar field interactions with the solar plasma, Proc. of the Third Lunar Science Conf., Vol. 3, The M. I. T. Press, in press, 1972.

Ness, N. F., K. W. Behannon, C. S. Scearce, and S. C. Cartarano, Early results from the magnetic field experiment on Lunar Explorer 35, J. Geophys. Res., 72, 5769-5778, 1967.

Schubert, G., and D. S. Colburn, Thin highly conducting layer in the Moon: Consistent interpretation of day side and night side electromagnetic responses, J. Geophys. Res., 76, 8174-8180, 1971.

Schubert, G., and K. Schwartz, High frequency electromagnetic response of the Moon, J. Geophys. Res., 77, 76-83, 1972.

Schubert, G., C. P. Sonett, K. Schwartz, and H. J. Lee, The induced magnetosphere of the Moon - I. Theory, submitted to J. Geophys. Res., 1972.

Sill, W. R., Lunar conductivity models from the Apollo 12 magnetometer experiment, The Moon, 4, 3-17, 1972.

Smith, B. F., D. S. Colburn, G. Schubert, K. Schwartz, and C. P. Sonett, The induced magnetosphere of the Moon - II. Experiment, in preparation, 1972.

Sonett, C. P., and D. S. Colburn, Establishment of a lunar unipolar generator and associated shock and wake in the solar wind, Nature, 216, 340-343, 1967.

Sonett, C. P., D. S. Colburn, P. Dyal, C. W. Parkin, B. F. Smith, G. Schubert, and K. Schwartz, Lunar electrical conductivity profile, Nature, 230, 359-362, 1971a.

Sonett, C. P., D. S. Colburn, G. Schubert, B. F. Smith, and K. Schwartz, Lunar electrical conductivity from Apollo 12 magnetometer measuremens: Compositional and thermal inferences, Proc. of the Second Lunar Science Conf., Vol. 3, 2415-2431, The M. I. T. Press, 1971b.

Sonett, C. P., P. Dyal, C. W. Parkin, D. S. Colburn, J. D. Mihalov, and B. F. Smith, Whole body response of the Moon to electromagnetic induction by the solar wind, Science, 172, 256-258, 1971c.

Sonett, C. P., B. F. Smith, D. S. Colburn, G. Schubert, and K. Schwartz, The induced magnetic field of the Moon: Conductivity profiles and inferred temperature, Proc. of the Third Lunar Science Conf., Vol. 3, The M. I. T. Press, in press, 1972.

FIGURE CAPTIONS

Figure 1

Lunar dark side transfer functions, A_x - o (vertical), A_y - Δ (east-west) and A_z - □ (north-south) in the frequency interval 1.7×10^{-3} to 3×10^{-2} Hz based on six hours of time series records from Explorer 35 and Apollo 12 lunar surface magnetometers. LSM is within 45^{o} of the antisolar point. Each data point and error estimate are the mean and standard deviation of the means, respectively, of individual 1 hour time series transfer functions.

Figure 2

Radial and tangential vacuum transfer functions for uniformly conducting Moon models (solid lines) and for models with perfectly conducting cores of radius b surrounded by insulating shells of thickness a-b (horizontal dashed lines). The data of Figure 1 is included. The observed low frequency tangential amplification exceeds the limit of 1.5 for any spherical body scattering radiation in vacuum.

Figure 3

The calculated radial response derived from vacuum inversion of A_x data into a model conductivity profile is shown superimposed upon the radial data.

The upper solid line shows the forward calculated vacuum tangential response based upon the conductivity model obtained from the radial inversion. Night side tangential amplification data are far in excess of the theoretical vacuum prediction. The additional amplification is due to cavity confinement of scattered radiation. The vacuum derived conductivity model cannot even qualitatively simultaneously satisfy both radial and tangential data.

Figure 4

The effect on the vacuum radial response of adding progressively larger cores of conductivity 10^{-2}mhos/m to an otherwise uniform Moon of conductivity 1.7×10^{-4}mhos/m. The equally satisfactory fit of the uniform model and the one with a 1000 km core to the A_x data shows that such a core is not resolvable from the A_x data using vacuum scattering theory. A 1200 km core would begin to be resolvable, but the inclusion of such a core would not improve the overall fit.

Figure 5

The effect on the vacuum radial response of adding progressively thicker insulating outer shells to an otherwise uniform Moon with $\sigma = 1.7\times10^{-4}$mhos/m. A nonconducting crust 100 km thick is barely resolvable from the data using vacuum scattering theory.

Figure 6

Forward calculations of transfer functions for the radial and tangential fields using a quasivacuum theory where the incident wave phase speed is based upon a field of Alfvén waves convecting in the solar wind and propagating along the mean Parker spiral direction. The effects of quadrupole and higher orders is seen at the high frequency end of the spectrum. The angle θ is the scattering angle between the radius vector from the center of the Moon to the position of the surface magnetometer and the incident wave vector. Note that the scattering parameter ($2\pi a/\lambda$) assigns a major fraction of lunar electromagnetic scattering to the Mie regime. These calculations are based upon the iterated conductivity model reported in the text.

Figure 7

Vacuum radial transfer functions for conductivity models derived by Dyal and Parkin (1971b) (Model D1) and Dyal et al. (1972) (Model D2) from analysis of individual night side transient events. The conductivity models are quantitatively described in the text. Also shown is the effect on the response of reducing the core conductivities holding other model parameters fixed. A highly conducting core is not resolvable and is not required to match the long time behavior of the Moon.

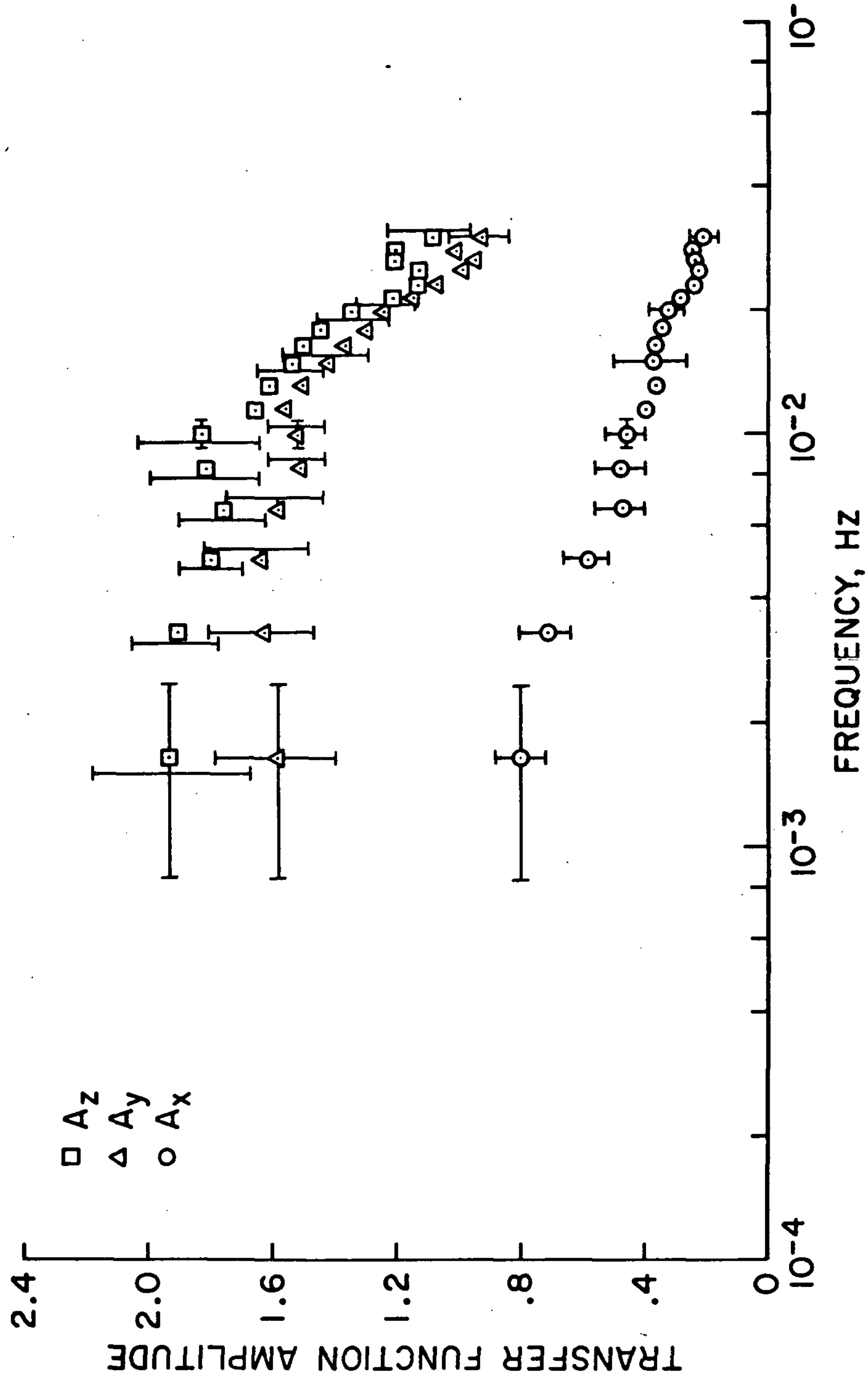

□ A_z
△ A_y
○ A_x
TRANSFER FUNCTION AMPLITUDE
0
.4
.8
1.2
1.6
2.0
2.4
10^{-4}
10^{-3}
10^{-2}
10^{-1}
FREQUENCY, Hz

Fig 1

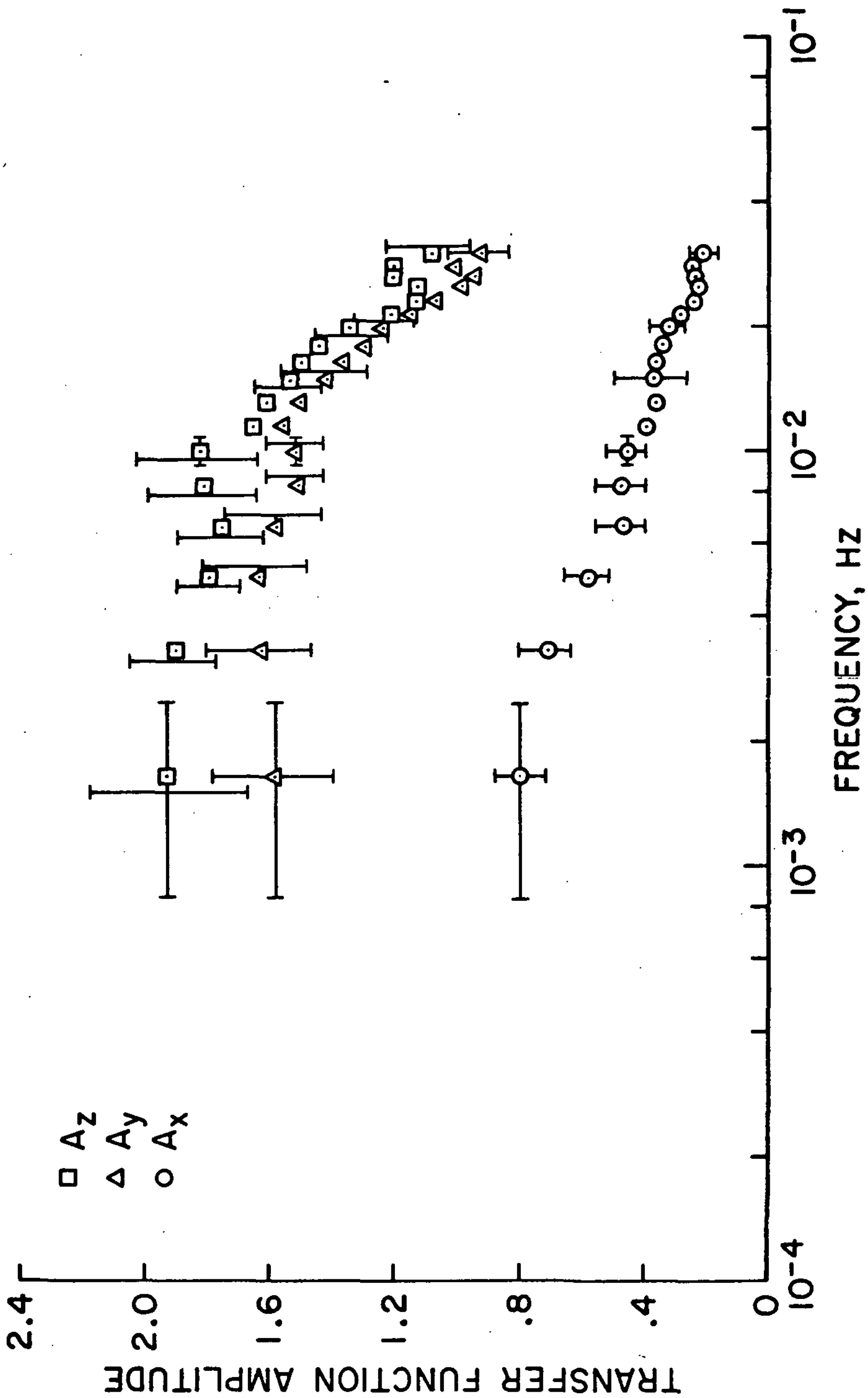

□ Az
△ Ay
○ Ax
TRANSFER FUNCTION AMPLITUDE
2.4
2.0
1.6
1.2
.8
.4
0
10-4
10-3
10-2
10-1
FREQUENCY, HZ

Fig 1

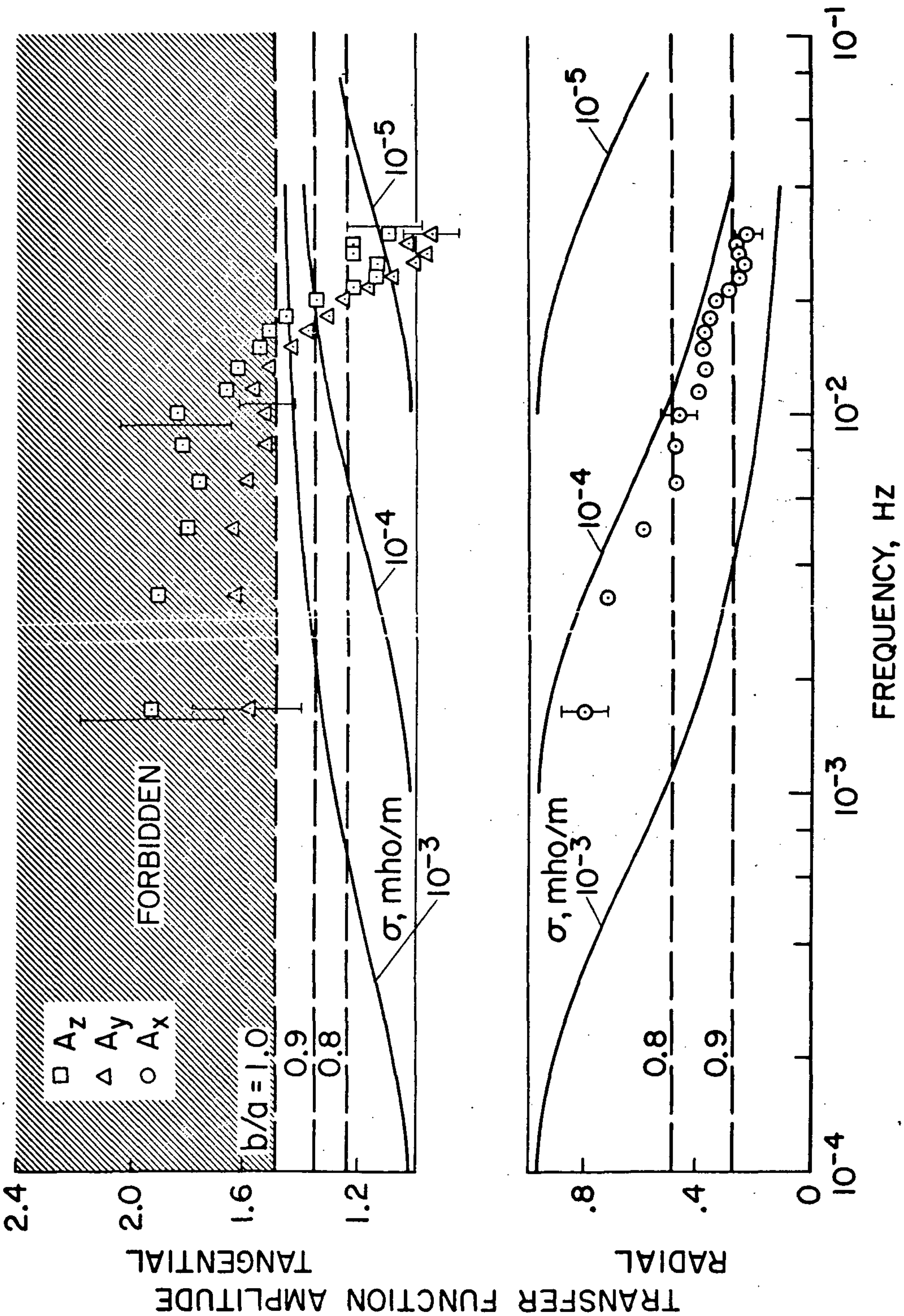
TRANSFER FUNCTION AMPLITUDE
TANGENTIAL
RADIAL
FREQUENCY, Hz
FORBIDDEN
□ A_z
△ A_y
○ A_x
b/a = 1.0
0.9
0.8
σ, mho/m
10^{-3}
10^{-4}
10^{-5}
10^{-1}
10^{-2}
2.4
2.0
1.6
1.2
.8
.4
0

Fig. 2

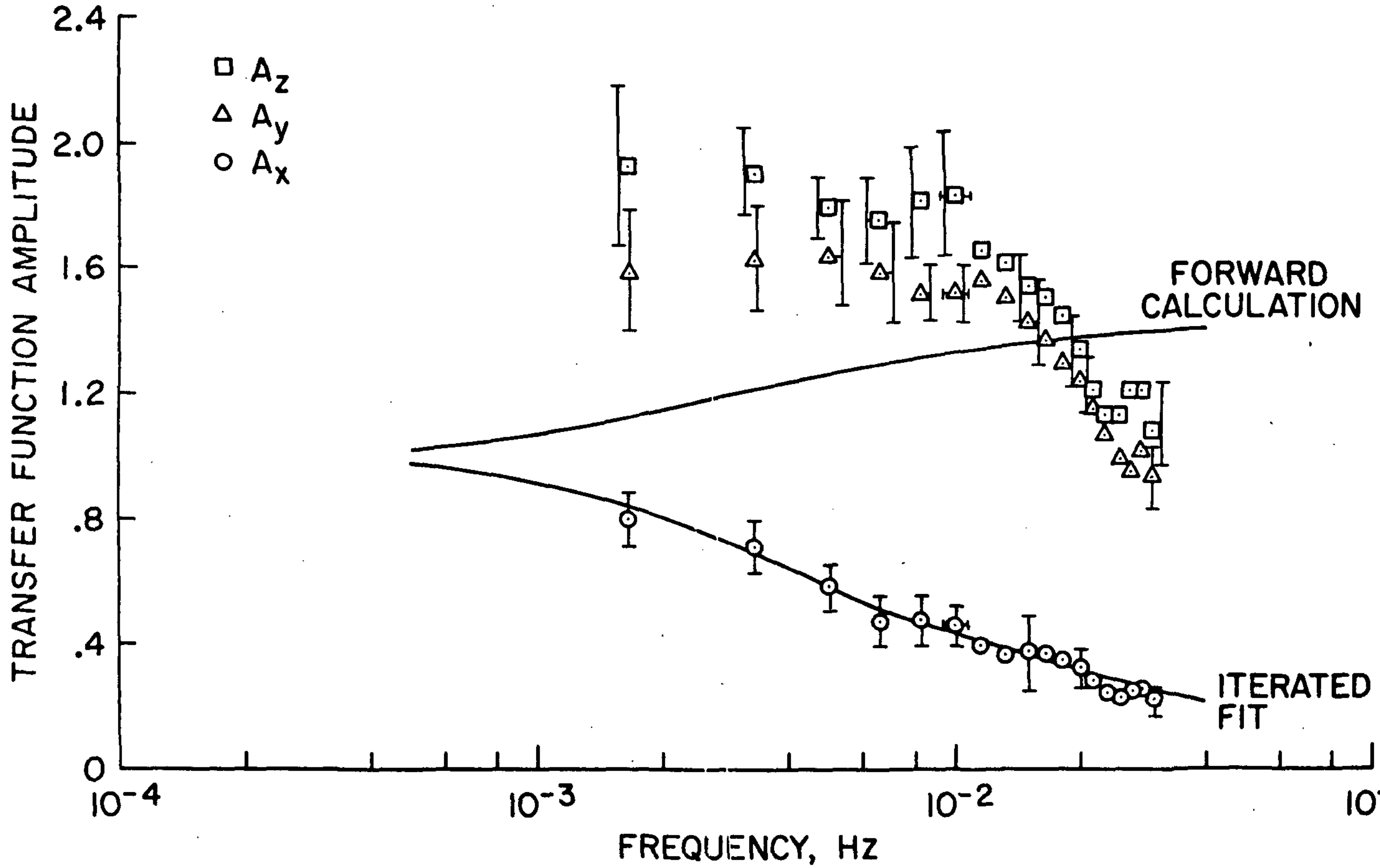
TRANSFER FUNCTION AMPLITUDE
2.4
2.0
1.6
1.2
.8
.4
0
A_z
A_y
A_x
FORWARD CALCULATION
ITERATED FIT
10^{-4}
10^{-3}
10^{-2}
10^{-1}
FREQUENCY, Hz

Fig. 3

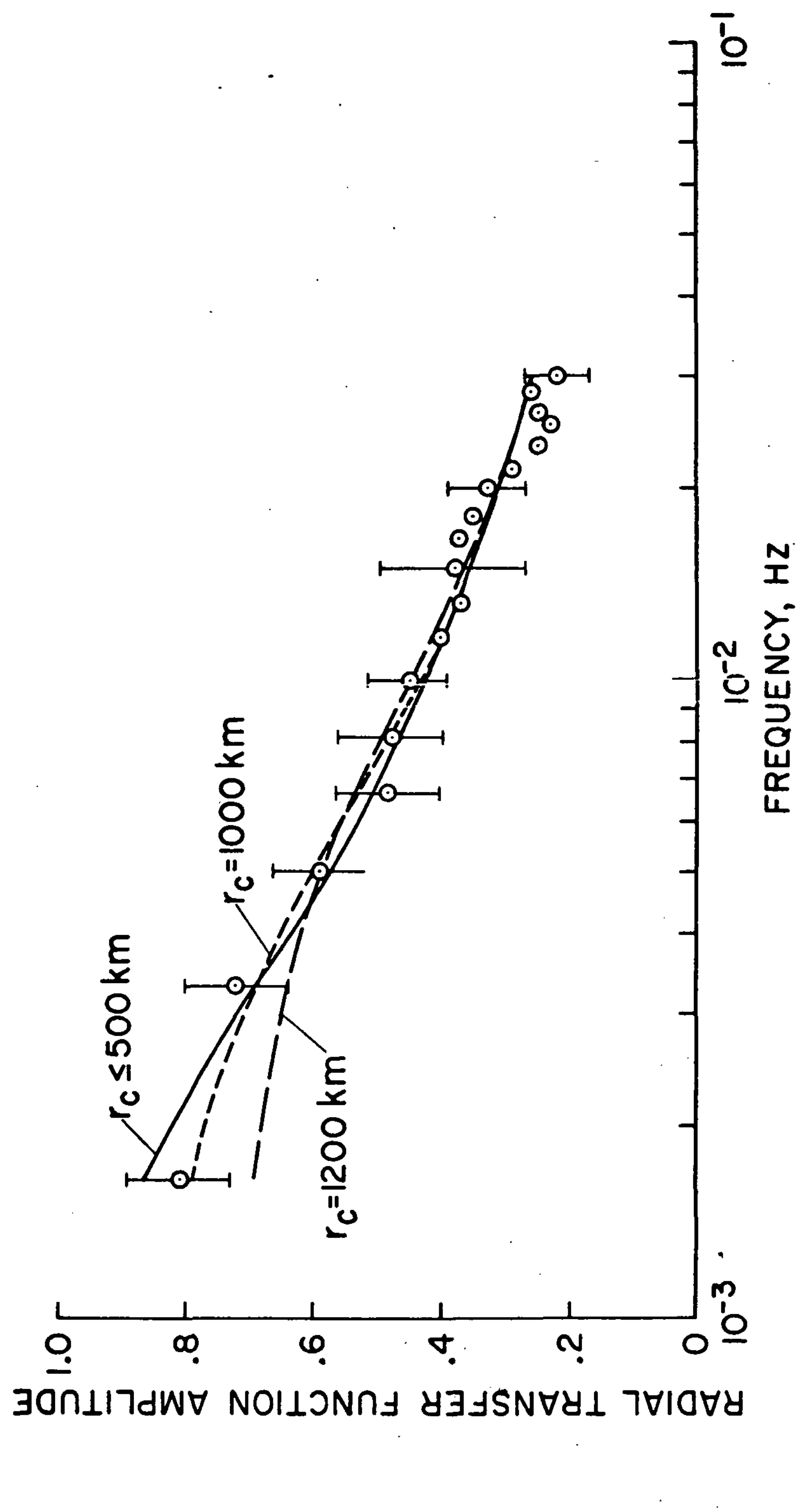
RADIAL TRANSFER FUNCTION AMPLITUDE
FREQUENCY, HZ
1.0
.8
.6
.4
.2
0
10^{-3}
10^{-2}
10^{-1}
$r_c \leq 500$ km
r_c=1000 km
r_c=1200 km

Fig. 4

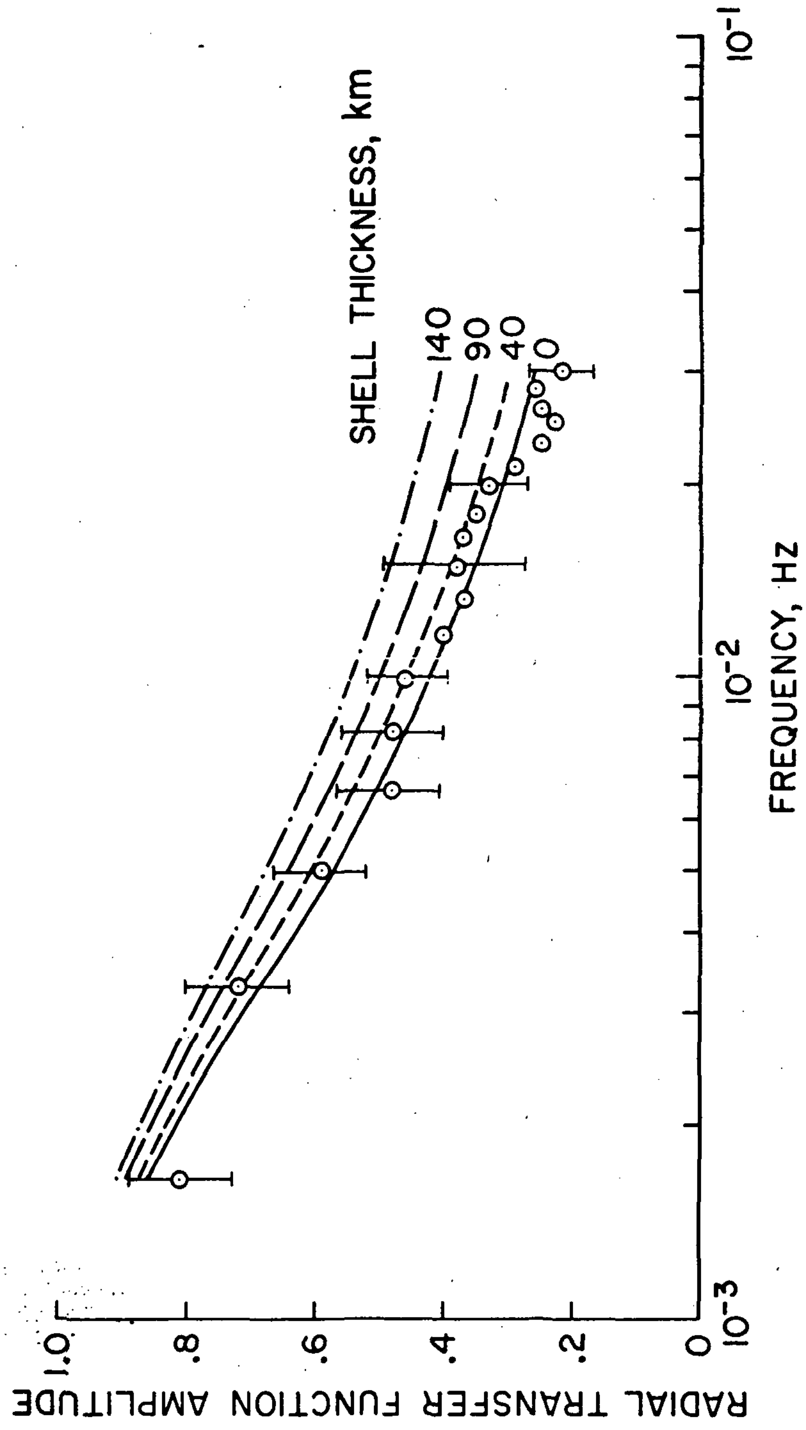
SHELL THICKNESS, km
140
90
40
0
FREQUENCY, Hz
RADIAL TRANSFER FUNCTION AMPLITUDE
1.0
.8
.6
.4
.2
0
10^{-3}
10^{-2}
10^{-1}

Fig. 5

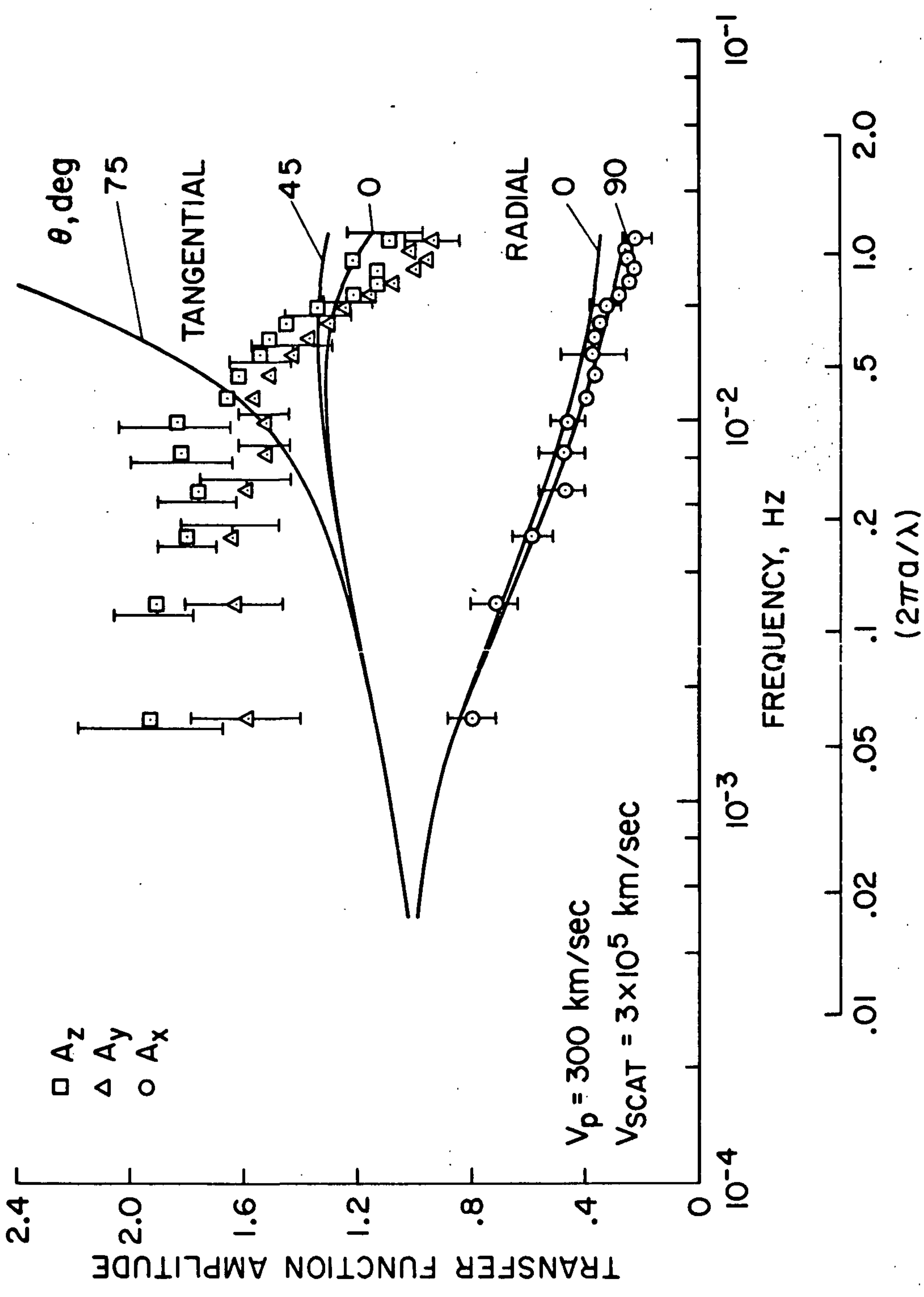
TRANSFER FUNCTION AMPLITUDE
2.4
2.0
1.6
1.2
.8
.4
0
10^{-4}
10^{-3}
10^{-2}
10^{-1}
FREQUENCY, Hz
.01
.02
.05
.1
.2
.5
1.0
2.0
$(2\pi a/\lambda)$
A_z
A_y
A_x
V_p = 300 km/sec
V_{SCAT} = 3×10^5 km/sec
θ, deg
75
45
0
TANGENTIAL
RADIAL
0
90

Fig. 5

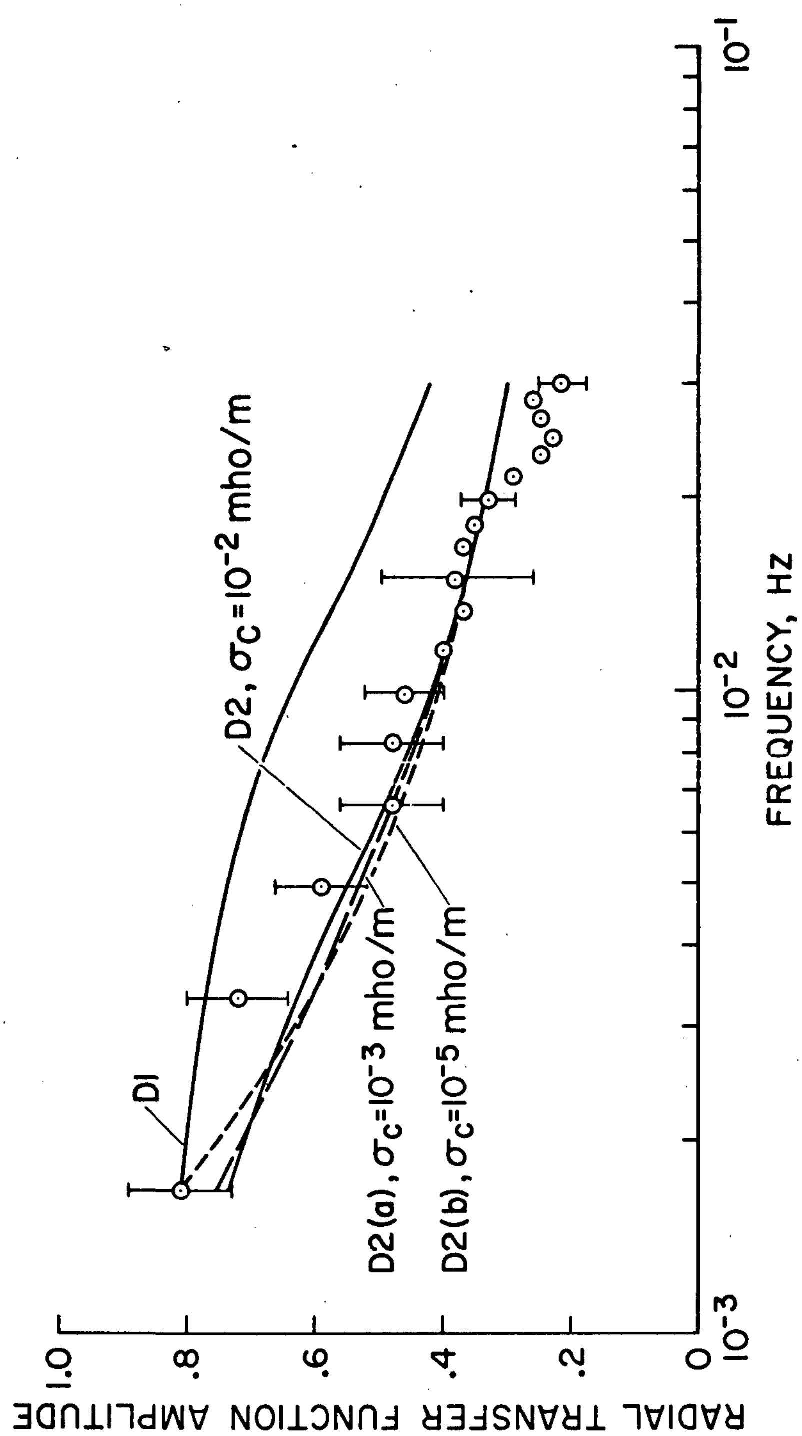
RADIAL TRANSFER FUNCTION AMPLITUDE
0
.2
.4
.6
.8
1.0
FREQUENCY, Hz
10^{-3}
10^{-2}
10^{-1}
D1
D2, $\sigma_C = 10^{-2}$ mho/m
D2(a), $\sigma_C = 10^{-3}$ mho/m
D2(b), $\sigma_C = 10^{-5}$ mho/m

Fig. 7